Photosynth Res (2016) 127:13–24
DOI 10.1007/s11120-014-0068-7

REGULAR PAPER

Connectivity of the intracytoplasmic membrane of *Rhodobacter sphaeroides*: a functional approach

André Verméglio · Jérôme Lavergne · Fabrice Rappaport

Received: 5 November 2014 / Accepted: 9 December 2014 / Published online: 16 December 2014

Abstract The photosynthetic apparatus in the bacterium *Rhodobacter sphaeroides* is mostly present in intracytoplasmic membrane invaginations. It has long been debated whether these invaginations remain in topological continuity with the cytoplasmic membrane, or form isolated chromatophore vesicles. This issue is revisited here by functional approaches. The ionophore gramicidin was used as a probe of the relative size of the electro-osmotic units in isolated chromatophores, spheroplasts, or intact cells. The decay of the membrane potential was monitored from the electrochromic shift of carotenoids. The half-time of the decay induced by a single channel in intact cells was about 6 ms, thus three orders of magnitude slower than in isolated chromatophores. In spheroplasts obtained by lysis of the cell wall, the single channel decay was still slower (~23 ms) and the sensitivity toward the gramicidin concentration was enhanced 1,000-fold with respect to isolated chromatophores. These results indicate that the area of the functional membrane in cells or spheroplasts is about three orders of magnitude larger than that of isolated chromatophores. Intracytoplasmic vesicles, if present, could contribute to at most 10 % of the photosynthetic apparatus in intact cells of *Rba. sphaeroides*. Similar conclusions were obtained from the effect of a ΔpH-induced diffusion potential in intact cells. This caused a large electrochromic response of carotenoids, of similar amplitude as the light-induced change, indicating that most of the system is sensitive to a pH change of the external medium. A single internal membrane and periplasmic space may offer significant advantages concerning renewal of the photosynthetic apparatus and reallocation of the components shared with other bioenergetic pathways.

Keywords *Rhodobacter sphaeroides* · Intracytoplasmic membrane structure · Membrane potential · Gramicidin

Abbreviations

CCCP	Carbonyl cyanide *m*-chlorophenylhydrazone
CM	Cytoplasmic membrane
FCCP	Carbonyl-*p*-trifluoromethoxyphenylhydrazone
ICM	Intracytoplasmic membrane
Rba	*Rhodobacter*
RC	Reaction center

Introduction

The intracytoplasmic membrane (ICM) of the purple bacterium *Rhodobacter* (*Rba.*) *sphaeroides* contains all of the components required for performing anaerobic photosynthesis, viz. light-harvesting complexes, electron transfer complexes (reaction center and the cytochrome bc_1

A. Verméglio (✉) · J. Lavergne
CEA, IBEB, Laboratoire de Bioénergétique Cellulaire, 13108 Saint-Paul-Lez-Durance, France
e-mail: avermeglio@cea.fr; andre.vermeglio@cea.fr

A. Verméglio · J. Lavergne
CNRS, UMR 7265 Biol Veget & Microbiol Environ, 13108 Saint-Paul-Lez-Durance, France

A. Verméglio · J. Lavergne
Aix Marseille Université, BVME UMR7265, 13284 Marseille, France

F. Rappaport
Institut de Biologie Physico-Chimique, UMR 7141 CNRS-UPMC, 13, rue Pierre et Marie Curie, 75005 Paris, France

complex), electron transfer shuttles (quinones and cytochrome c_2), and the ATP-synthase. Typically, incident light is captured by carotenoid and bacteriochlorophyll molecules non-covalently bound to the light-harvesting complexes LH1 and LH2. This excitation energy is transferred within the network of light-harvesting complexes until it eventually reaches, on a time scale of picoseconds, the photosynthetic reaction center (RC). At this level, a charge separation occurs between the primary donor, a special pair of bacteriochlorophyll molecules, and a quinone molecule named Q_A. The electron is then transferred to a second quinone molecule, Q_B. After two photochemical turnovers, Q_B is fully reduced and protonated, taking up two protons from the cytoplasmic phase. This quinol diffuses out of the RC and donates its electrons to the cytochrome bc_1 complex where the Q-cycle occurs. The ultimate products of the Q-cycle are (on a basis of two photochemical turnovers in the RC) four protons entering the periplasmic space, two protons taken from the cytoplasmic space and the transfer of two electrons back to the RC via cytochrome c_2. This reduction completes the light-induced cyclic electron transfer found in all purple photosynthetic bacteria where the proton-motive force generated between the periplasmic and cytoplasmic phases is utilized for ATP synthesis (see e.g., Hunter et al. 2009). In addition to the photosynthetic apparatus, *Rba. sphaeroides* develops the numerous components necessary for bioenergetic processes such as respiration or even denitrification in the case *Rba. sphaeroides* forma sp. *denitrificans* (Satoh 1977). These bioenergetics chains use not only specific enzymes but also electrons carriers identical to those involved in the photosynthetic apparatus (Ubiquinone, cytochrome bc_1 complex, or cytochrome c_2). While the photosynthetic apparatus is mostly present in the ICM invaginations, the other chains are predominantly found in the smooth regions of the cytoplasmic membrane.

The topology of the ICM has long been debated. In the early fifties, isolated ICM (or chromatophores) of *Rhodospirillum rubrum* was shown to contain the photosynthetic apparatus and to be able to carry out photophosphorylation in the presence of ADP and pyrophosphate (Pardee et al. 1952; Frenkel 1954). From their first observations of chromatophores in intact cells of *Rba. sphaeroides* and *R. rubrum* by electron microscopy, Vatter and Wolfe (1958) inferred that these vesicles were isolated rather than continuous to the cytoplasmic membrane. In subsequent works, however, it was found that the vesicles protrude from the ICM to which they remain attached and form a branched chromatophore network in topological continuity with the cytoplasmic membrane (Cohen-Bazire and Kunisawa 1962; Holt and Marr 1965). According to this view, there is a unique periplasmic phase in the cell, common to all bioenergetic chains.

Besides these electron microscopy data, the strong inhibition by light of both respiratory activity (Nakamura 1937; Van Niel 1941) and nitrate reduction (Satoh 1977; McEwan et al. 1982) indicates direct interaction between these two light-independent bioenergetic processes and photosynthesis. This inhibition is caused by two concurrent mechanisms. First, there is a thermodynamic control by the light-induced proton-motive force on the proton-translocating complexes involved in the electron flow (i.e., dehydrogenases and cytochrome bc_1 complex) (Cotton et al. 1983; McEwan et al. 1984). The second mechanism is a competition between redox components shared by the respiratory (or denitrification) and photosynthetic chains (i.e., ubiquinone, cytochrome bc_1 complex, and cytochrome c_2), which results in a shortage of electrons available to the respiratory and denitrification pathways (Richaud et al. 1986; Rugolo and Zannoni 1983; Sabaty et al. 1993). Although this photoinhibition of respiration or denitrification implies a significant sharing of components in the periplasmic space and within the membrane by the three bioenergetic processes (photosynthesis, respiration, and denitrification), it does not exclude that part of the photosynthetic chains could be completely separated from the respiratory and denitrification chains.

Another indication that respiratory and photosynthetic elements share the same membrane is the large carotenoid band-shift induced by the respiratory activity. This spectral shift is an electrochromic response of carotenoids from the light-harvesting complexes (those belonging to the LH2), known to be a linear indicator of the membrane electric potential. The amplitude of the carotenoid signal associated with the membrane potential sustained by respiration is typically $\geq$80 % of the amplitude observed under a continuous illumination, implying that at least a large fraction of the electrochromic probes feel the membrane potential generated by respiration (see Fig. 7 in the present paper for an example). Finally, the observation by Prince et al. (1975) that the digestion of the external membrane when preparing spheroplasts results in the outflow of most of cytochrome c_2 is a strong further evidence for the topological uniqueness of the periplasmic space and connectivity within the ICM.

This view has prevailed during the last four decades until Tucker and co-workers (2010) using cryo-electron tomography revealed a more complex situation in *Rba. sphaeroides*. They identified, on the one hand, structures which retained a connection with the cytoplasmic membrane and, on the other hand, organelles completely separated from this membrane. This tomography methodology does not permit, however, a precise quantification of the relative amount of these isolated organelles. In a commentary paper on this work, Niederman (2010) placed the emphasis on the detached chromatophores, the formation

of which "is shown to represent the final stage in a membrane invagination and growth process". More recently, however, Scheuring et al. (2014) using a similar approach concluded that the ICM of *Rba. sphaeroides* form a continuous reticulum with no detached vesicles.

In this context, it may be useful to gain additional information on the functional stakes involved in this debate. In the present work, we address this subject by estimating the size of the membrane subjected to the photo-induced electro-osmotic effect in intact cells of *Rba. sphaeroides*. In a first approach, we used the ionophore gramicidin, which causes conspicuous effects even when present as a single channel per vesicle. A second approach deals with the diffusion potential induced by a ΔpH.

Materials and methods

Bacterial growth

Rhodobacter sphaeroides Ga cells were grown in the light in Hutner medium at 30 °C under anaerobic conditions under incandescent lamps (75 μE m^{-2} s^{-1}).

Spheroplasts and chromatophore preparation

Spheroplasts were prepared by incubating cells in 50 mM Tris–HCl (pH 8) in the presence of 0.45 M sucrose, 1.3 mM EDTA, and 0.6 mg/ml lysozyme at 30 °C. After 60 min incubation, the suspension was centrifuged for 20 min at 4,000×*g* and the pellet was resuspended in 0.45 M sucrose, 50 mM Tris–HCl (pH 8).

Chromatophores were prepared according to Baccarini-Melandri and Melandri (1971). The cells were broken in a French press at 16,000 psi. The unbroken material was eliminated by a 20,000×*g* centrifugation (20 min). The supernatant was then spun at 200,000×*g* for 90 min. The pellet was resuspended in a glycylglycine buffer (50 mM, pH 7.2), centrifuged again and finally resuspended in 100 mM glycylglycine buffer (pH 7.2) with an equal volume of glycerol for storage at −80 °C.

Absorbance change measurements

Light-induced absorbance changes in the range from 10 μs to several seconds were measured with an apparatus derived from the one described by Joliot et al. (1980), with modifications as described by de Rivoyre et al. (2010). In this machine, the absorption changes are sampled at discrete times using monochromatic flashes of a few μs duration. Kinetics of the carotenoid band-shift (or membrane potential) was measured as the difference $\Delta A_{505\ nm} - \Delta A_{490\ nm}$.

Difference absorption spectra in the dark (as shown in Fig. 7) were acquired using the same machine, with programmed wavelength scanning (3 detector flashes at 10 Hz at each selected wavelength) and automatic gain adjustment. The sample in the reference cuvette was left unmodified and successive difference spectra were calculated to monitor the changes occurring in the reference sample.

Kinetic measurements at sub-μs resolution were carried out with another lab-built spectrophotometer (Béal et al. 1999) where the absorption changes are sampled with flashes of ns duration. These flashes were provided by a neodymium:yttrium–aluminum garnet (Nd:YAG, 355 nm) pumped optical parametric oscillator, which produces monochromatic flashes (1 nm full-width at half-maximum) with a duration of 5 ns. Excitation was provided by a second Nd:YAG (532 nm) pumped optical parametric oscillator, which produces monochromatic saturating flashes at 800 nm (1 nm full-width at half-maximum) with a duration of 5 ns.

Kinetics of the membrane potential decay in the presence of gramicidin

We used the equations derived by Althoff et al. (1991), assuming a Poisson distribution of the gramicidin channels among a population of vesicles with fixed size. If m is the average number of channels per vesicle, the fraction of vesicles with n channels is

$$P(n,m) = \frac{e^{-m}m^n}{n!} \quad (1)$$

Assuming that the decay in a vesicle containing n channels is an exponential with rate constant $n \times k_{sc}$ (where k_{sc} is the rate constant for a single channel), the overall kinetics is then:

$$F(t,m) = \sum_{n=1}^{\infty} P(n,m)\ e^{-nk_{sc}t} \quad (2)$$

This may be recast (as may be checked by noting that Σ $(x^n/n!)$ is the Taylor series for e^x) into the compact form:

$$F(t,m) = e^{-m}\left(e^{m\exp(-k_{sc}t)} - 1\right) \quad (3)$$

Results and discussion

Effect of gramicidin on chromatophores, intact cells and spheroplasts from *Rba. sphaeroides*

Althoff et al. (1991) observed that, in the presence of subsaturating concentrations of gramicidin, the decrease of the light-induced membrane potential of isolated chromatophores is heterogeneous, with a fast phase in the μs time

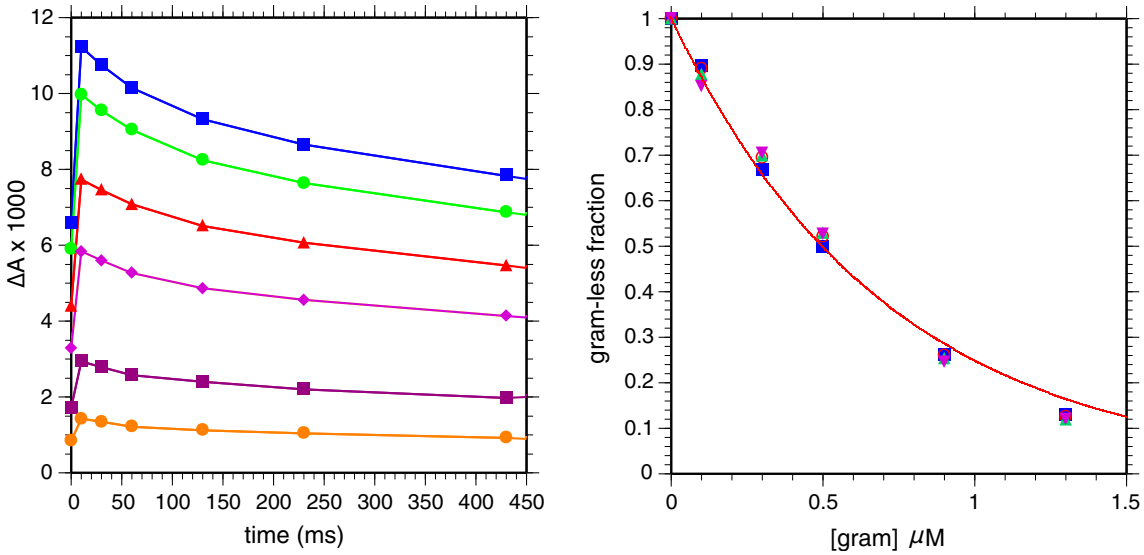

Fig. 1 Effect of a range of gramicidin concentrations on the kinetics of the carotenoid band-shift following a single turnover flash in chromatophores of *Rba. sphaeroides*. *Left panel* kinetic data points sampled at discrete times were joined by straight lines. From *top to bottom*, the gramicidin concentration was 0 (control), 100, 300, 500, 900, 1300 nM. The first datapoint is at 30 μs, thus after the completion of the fast decay phase shown in Fig. 2. *Right panel* relative amplitude of the kinetics shown in the *left panel* as a function of the concentration of gramicidin. At each concentration, the ratio with respect to the control was plotted for 4 kinetic datapoints (30 μs, 30, 430 ms, and 1.63 s). The values thus obtained are superimposed showing that the kinetics are homothetic. The *line* is an exponential fit with a half-effect concentration of 493 nM

scale and a slow phase. The relative amplitude of the fast phase increases with the concentration of added gramicidin up to 100 %, while its rate increases. The kinetics of the slow phase is unmodified with respect to that observed in the absence of ionophore, but for an amplitude factor. The fast phase was ascribed to the binding of gramicidin in a fraction of the chromatophores while the slow phase corresponds to chromatophores which remain devoid of ionophore. The number of gramicidin channels per vesicle is expected to follow a Poisson distribution. According to Althoff et al.'s analysis, the presence of a single channel of gramicidin in a chromatophore induces an exponential decay of the membrane potential with half-time ~5 μs and chromatophores endowed with 2, 3… channels display a 2-, 3-…-fold accelerated decay with respect to the single channel case (see Eqs. 1–3 in "Methods" section).

Based on the above findings, we reasoned that gramicidin could provide a valuable tool for investigating the size of the electro-osmotic unit(s) present in intact cells. The decay of the membrane potential can be seen as the discharge of a capacitor, with a time constant equal to the product RC (where R is the membrane resistance and C the membrane capacitance). Assuming that the conductance of the individual gramicidin channel does not depend on the vesicle size, the decay rate is then expected to be proportional to C^{-1} and therefore to S^{-1} (where S is the membrane area of the vesicle). Furthermore, the capture efficiency of the vesicle toward gramicidin should be proportional to its area. Thus, if it turns out that the cell of *Rba. sphaeroides* possesses a single membrane which area is, say, 1000 times larger than the area of one chromatophore, one expects a 1,000-fold slower decay rate caused by a single channel (i.e., in the ms range) and a 1,000-fold enhanced sensitivity to the concentration of added gramicidin.

Chromatophores

In a first step, we reproduced the experiments of Althoff et al. (1991). Figure 1, left panel, shows the amplitude of the flash-induced carotenoid band-shift measured in a suspension of *Rba. sphaeroides* chromatophores for a concentration range of gramicidin. The two first kinetic data points shown in these traces are located at 30 μs and 10 ms. In the absence of gramicidin, the amplitude of the signal at 30 μs is predominantly due to the membrane potential generated by charge separation in the RC, while the subsequent rise (10 ms point) is due to the electrogenic events (Q-cycle) occurring in the cytochrome bc_1 complex. This is followed by a decay corresponding to the ionic conductance of the membrane. Gramicidin appears to cause a decrease in the amplitude of the kinetics, but their time course is not affected in the time range extending from 30 μs to several seconds, as illustrated by the superimposed ratios plotted in the right hand panel. The diminished amplitude is not due to an inhibition of the photochemical

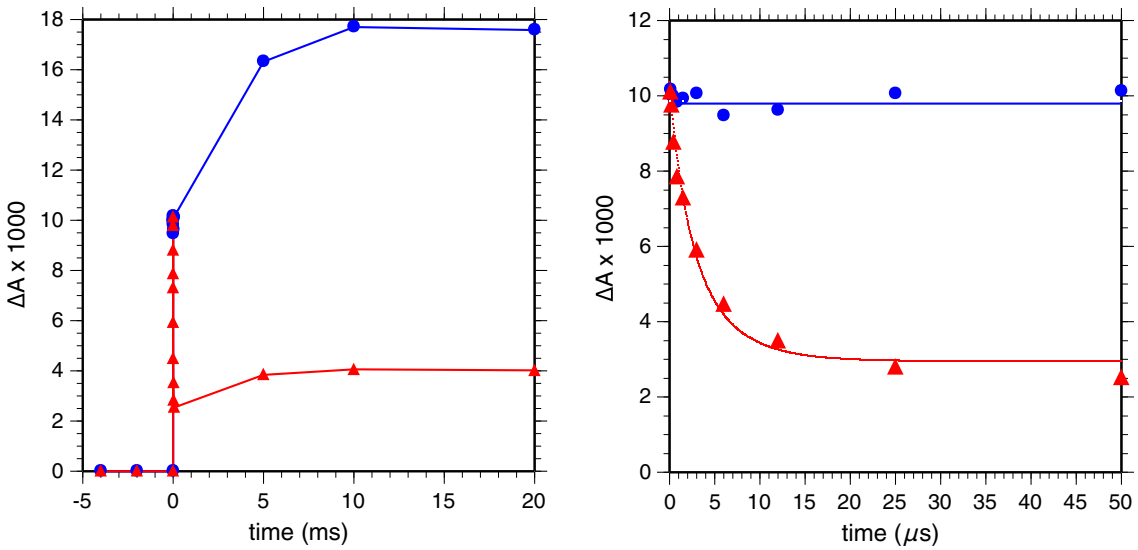

Fig. 2 Kinetics of the carotenoid band-shift induced by a 5-ns saturating flash in chromatophores at sub-μs time resolution. The traces were plotted on a ms scale (*left*) and μs scale (*right*). *Blue line* and *circles*, control without gramicidin; *red line* and *triangles*, gramicidin at 5.3 μM. The *red curve* in the *right hand panel* is a fit with Eq. 3, yielding $m = 1.27$ (average number of channels per vesicle) and $k_{sc} = 209\ ms^{-1}$ (or $t_{1/2,sc} = 3.3\ \mu s$)

activity, as was checked by monitoring absorption changes at wavelengths where the carotenoid shift does not contribute (e.g., 542 nm, not shown). The reason for this decrease becomes clear when resolving the kinetics of the carotenoid shift at shorter times, as illustrated in Fig. 2. In this experiment, the trace observed in the presence of 5.3 μM gramicidin displays a more than 4-fold reduction of its amplitude at times ≥20 μs (Fig. 2, left), which turns out to be entirely due to a rapid decay occurring in the μs range (Fig. 2, right). The initial amplitude, measured here at 100 ns, is the same as that of the control, confirming that the extent of charge separation is not affected by gramicidin (Fig. 2, right). The $t_{1/2}$ of the decay phase induced by the ionophore is ~2.1 μs. These findings are consistent with the interpretation put forward by Althoff et al. (1991). In this framework, the fast decay phase is due to vesicles which host one or more gramicidin channel(s), accounting here for 77 % of the total amplitude, while 23 % of the vesicles display unmodified kinetics. According to the Poisson distribution, a 23 % fraction of gramicidin-less vesicles imply that 34 % of the vesicles accommodate one channel, 25 % two channels, and so forth. When fitting the decay with the appropriate function (Eq. 3 in the "Methods" section), one obtains an estimate of the decay rate for a single channel, i.e., $k_{sc} = 0.21\ \mu s^{-1}$ (or $t_{1/2,sc} \approx 3.3\ \mu s$), in reasonable agreement with the value of $0.14 \pm 0.04\ \mu s^{-1}$ reported by Althoff et al. (1991).

Despite the overall agreement with the work of Althoff et al., there is a discrepancy concerning the concentration of gramicidin necessary to obtain a half saturated effect. In the experiments by Althoff et al. (1991), the half saturation was observed at 5 nM of gramicidin while in our hands it typically occurred around 500 nM (Fig. 1, right part). Part of the discrepancy is due to the higher chromatophore concentration in our experiments. Nevertheless, when expressed on the basis of the bacteriochlorophyll concentration we still have a 5–15 smaller sensitivity to gramicidin than reported in the previous work. We tested various preparations of chromatophores (including the same preparation procedure from Baccarini-Melandri and Melandri (1971) as in Althoff's work), used fresh samples of gramicidin and tried longer or more vigorous mixing procedures but this did not affect the results. As argued by Althoff et al. (1991) the concentration dependence found in their work was consistent with (i) a complete incorporation of the added gramicidin into the chromatophore membranes and (ii) a large association constant for the dimeric association of gramicidin monomers (required for channel formation). Thus, it seems that at least one of these requirements was not achieved in our hands. We have no explanation for this discrepancy.

In any case, our results support, as proposed by these authors, the presence of two populations of chromatophores at sub-saturating concentrations of gramicidin. Chromatophores devoid of gramicidin display unaffected kinetics of the membrane potential, while chromatophores endowed with one or several ionophore channels present a fast decay phase. This validates the use of gramicidin to determine the size of the functional membrane(s) in intact membranes of *Rba. sphaeroides*.

Intact cells

When intact cells of *Rba. sphaeroides* are placed under anaerobiosis, the decrease of the carotenoid band-shift induced by a single flash is slow because of the inactivation of the ATP-synthase. Due to the respiratory activity of the cells, the sample becomes anaerobic after its introduction in the closed cuvette, over a somewhat variable time that may last several tens of minutes. This process can be speeded up by addition of the mixture glucose–glucose oxidase (also adding catalase to eliminate H_2O_2), or of a small concentration of FCCP (0.1 μM). For convenience these procedures were used in some of our experiments and were found of no consequence as regards the effects of gramicidin described below.

The penetration of gramicidin into intact cells was not a straightforward matter. Long incubation times (several tens of minutes) were required to obtain an apparently stable effect. We observed a threshold behavior, with e.g., no observable effect at 1.3 μM gramicidin while a 2-fold larger concentration induced significant changes. More generally, the concentration dependence was rather erratic, i.e., not reproducible from one culture to another and even for the same culture during the experiment. To minimize this lack of reproducibility, the cells were incubated in the dark for several hours with various concentrations of gramicidin before measurements.

The results of such an experiment are shown in Fig. 3. Addition of gramicidin modifies the kinetics of the membrane potential at times ≤10 ms while the decay at longer times is not (or little, see below) affected, meaning that the amplitude is smaller, but the time course is homothetic. This suggests that, as noticed in the case of chromatophores, part of the cells have remained devoid of gramicidin. Another important point is that the amplitude of the membrane potential detected at 15 μs is not significantly affected by the addition of gramicidin. There was actually some scatter on this measurement, likely due to the long duration of the experiments. However, we made sure that no decay phase in the μs time-range was present (not shown), implying that no significant contribution of the type encountered with isolated chromatophores occurred. The kinetic changes caused by gramicidin thus appear located in the ms range. This is illustrated in Fig. 3, right part, as a plot of the differences between the kinetics of the membrane potential for various concentrations of gramicidin and those measured in the control experiment. The membrane potential decay caused by gramicidin appears in this plot as a rise phase at $t \leq 20$ ms. Since gramicidin affects the kinetics over the same time domain as the electrogenic events of the Q-cycle, one might suspect an inhibitory action on this process. We tested this possibility by using cells incubated with a saturating concentration of the bc_1 inhibitor myxothiazol (not shown). In these cells, the rise phase due to the Q-cycle is absent. Adding gramicidin in this material causes a membrane potential decay in the 10 ms time range, which appears more directly as a decay phase rather than an apparent suppression of the rise due to the Q-cycle. We conclude that the effect of gramicidin in cells can be ascribed to a *bona fide* ionophore effect rather than an inhibitory effect on the Q-cycle.

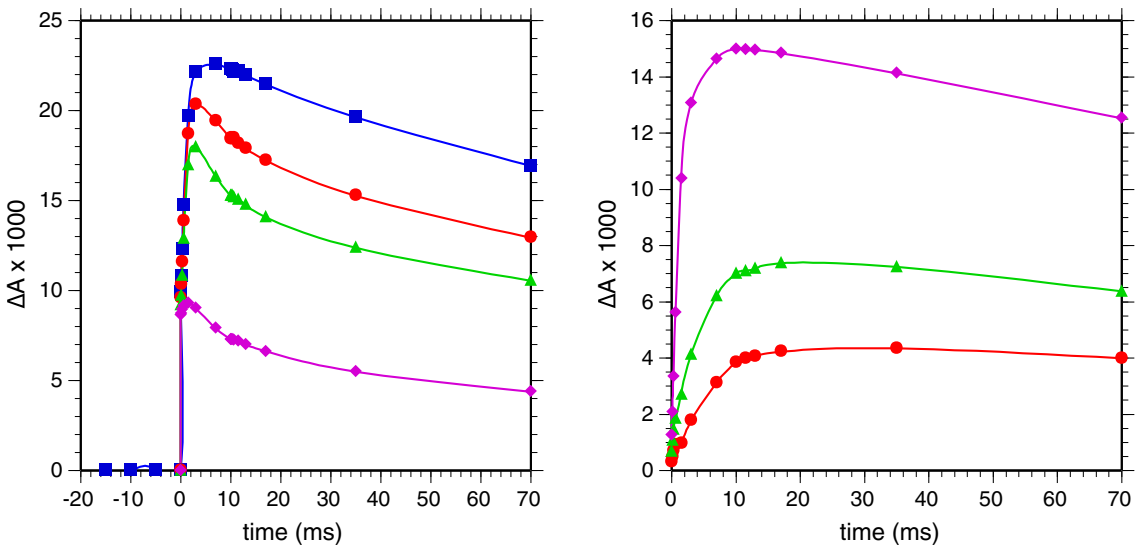

Fig. 3 Effect of a range of gramicidin concentrations on the kinetics of the carotenoid band-shift following a single turnover flash in intact cells of *Rba. sphaeroides* under anaerobic conditions. *Left panel*, kinetic traces for gramicidin concentrations (from *top to bottom*): 0 (control), 5, 10, and 20 μM. *Right panel*, the traces in the presence of gramicidin were subtracted from the control; from *top to bottom*, gramicidin 20, 10, and 5 μM

The rate of the leak created by the addition of gramicidin and its relative extent increased when increasing the gramicidin concentration (although not in a smooth and quantitatively reproducible way, as noticed earlier). In the experiment of Fig. 3, the half-time was 4.9 ms at 5 μM gramicidin, with 20 % of the cells contributing the fast phase (thus hosting one or more channels); it was 1 ms at 20 μM gramicidin, with 64 % of the cells affected. Using Eq. 3, one estimates that a single channel per cell will induce a decrease of the membrane potential with a half-time of about 6 ms. This half-time is about 1,800 times longer than the one measured in isolated chromatophores, implying a similar ratio between the chromatophore area and that of the functional membrane in intact cells of *Rba. sphaeroides*.

The concentrations of gramicidin required for observing these effects were, however, orders of magnitude larger than expected on the basis of a target membrane area 2,000-fold bigger than in isolated chromatophores. This is most probably related to the penetration difficulties mentioned earlier. Indeed, the half saturation effect occurred at about 10 μM in the experiments reported in Fig. 3, i.e., 20 times higher than for isolated chromatophores, while one would expect a sensitivity 2,000 times higher and thus a 2,000-fold smaller concentration at half saturation. The discrepancy is, therefore, by a factor of ~40,000. Clearly, the gramicidin concentration dependence in intact cells cannot provide any relevant information as to the issues under study, since it appears that a huge fraction of the ionophore is ineffective, probably due to the trapping of this chemical by other membranes or compounds present in the cells. A close comparison of the slow decay phases (in the seconds time range) in cell suspensions without or with gramicidin revealed a slight acceleration of the rate in the latter (e.g., when comparing the slopes for the same absolute amplitude of the carotenoid shift). This suggests that cells which did not possess a functional gramicidin channel when the flash was fired could gain one at later times, through a slow redistribution of the ionophore. This supports a homogeneous behavior rather than an interpretation implying populations of gramicidin sensitive and refractory cells. Irrespective of the problems raised by the massive sequestration of gramicidin in unknown cell components, the conclusions inferred from the kinetic observations remain relevant, i.e., that the decay phase in the 10 ms range corresponds to the leak induced by a few channel molecules in vesicles with an area bigger by about three orders of a magnitude than that of isolated chromatophores.

To circumvent the difficulties encountered with gramicidin penetration in intact cells, we studied the response of cells stripped from their outer membrane by lysozyme digestion, viz. spheroplasts.

Spheroplasts

Figure 4 shows the effect of various concentrations of gramicidin, from 200 pM to 10.5 nM, on the light-induced carotenoid band-shift in a suspension of spheroplasts in the presence of 1 mM sodium ascorbate. The absence of the ms rise phase related to the Q-cycle is due to the loss of cytochrome c_2. Indeed, no photo-oxidation of cytochrome c_2, measured at 551–542 nm, could be detected, indicating that less than ~5 % of the cytochrome c_2 was retained in our spheroplasts preparation. This is in good agreement with the results of Prince et al. (1975) who found also that at most 10 % of the cytochrome c_2 was photo-oxidized in their spheroplasts preparation compared to chromatophores. The kinetics were analyzed as illustrated in Fig. 5, for the addition of 500 pM gramicidin. The slow phase is homothetic to the time course of the control, with an amplitude factor of 0.37, implying that, at this concentration, 37 % of the spheroplasts have remained devoid of gramicidin. The kinetics of the other 63 %, which contain one or more channels, is obtained by subtraction. It decays with a halftime of 24 ms (right-hand panel). Fitting with Eq. 3, one estimates a single channel half-time of about 35 ms; taking into account 5 experiments, we obtained a range of 12–35 ms and an average of 23 ms. This is about 4-fold the half-time estimated for intact cells and 7,000-fold the half-time of chromatophores. The difference between spheroplasts and intact cells may be due to a modified capacitance caused by the changes of shape and/or ionic environment of the membrane.

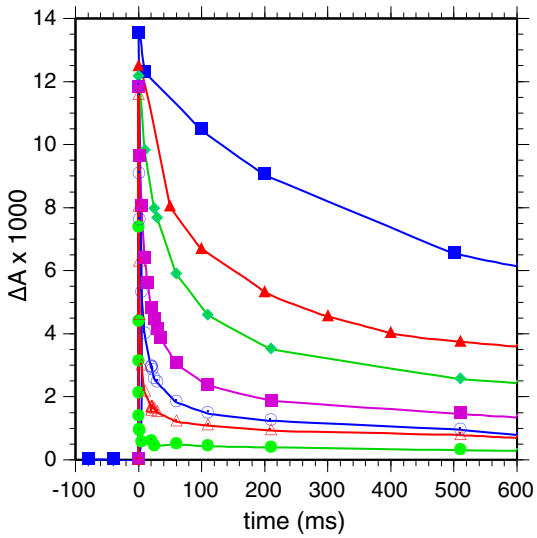

Fig. 4 Effect of a range of gramicidin concentrations on the kinetics of the carotenoid band-shift following a single turnover flash in spheroplasts from *Rba. sphaeroides*. The absence of the ms rise phase due to the Q-cycle is due to the loss of cytochrome c_2. The concentrations of gramicidin were, from *top to bottom* 0 (control), 200, 500 pM, 1.1, 5, 10.5 nM and 2 μM

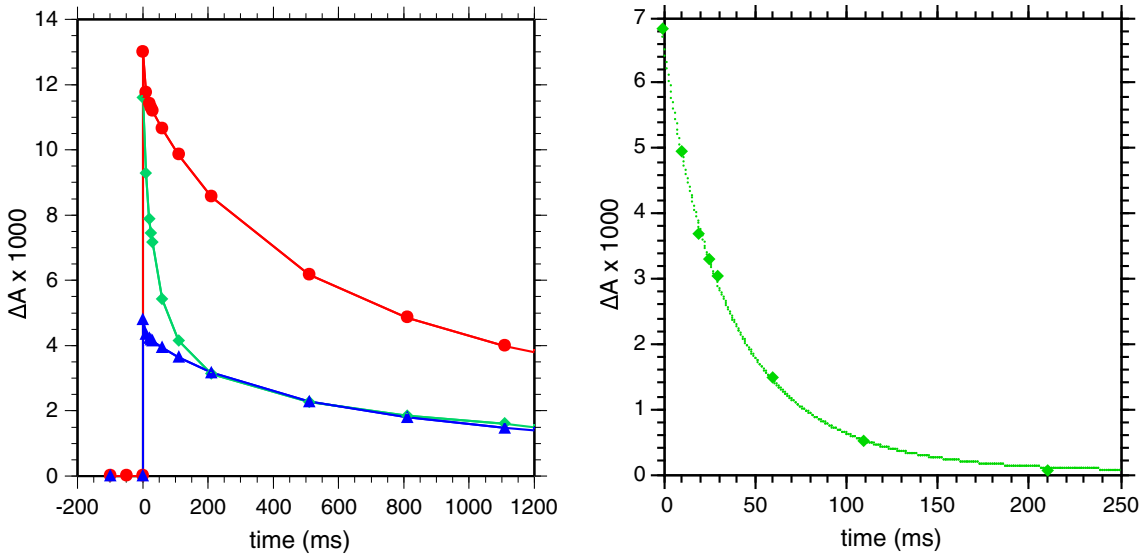

Fig. 5 Analysis of the decay induced by 500 pM gramicidin in spheroplasts. The *left panel* shows the control and 500 pM traces from Fig. 4. The *blue curve* is the control trace multiplied by 0.37 in order to match the slow phase of the 500 pM trace. The difference between the *green and blue curves* gives the decay due to gramicidin and was plotted in the *right hand panel*. The *line* is a fit with Eq. 3 (using $m = -\ln(0.37) \approx 1$), yielding $t_{1/2,sc} \approx 35$ ms

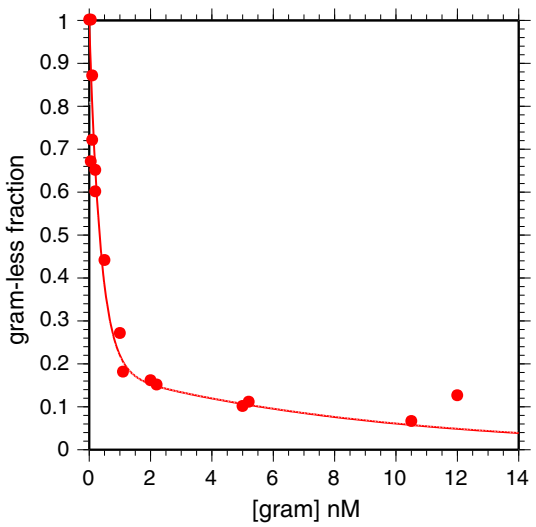

Fig. 6 Relative amplitude of the slow phase of the carotenoid change decay in spheroplasts as a function of the gramicidin concentration. This corresponds to the fraction of vesicles devoid of gramicidin. The *line* is a fit with a sum of two exponentials (data points at higher concentrations were taken into account), yielding $C_{1/2} = 254$ pM and 6.2 nM (for 81 and 19 % of the amplitude, respectively)

Figure 6 shows the concentration dependence of the gramicidin effect in spheroplasts. This represents a plot of the amplitude of the slow (unmodified) phase ascribed to the fraction of material devoid of gramicidin. The plot is biphasic with ~80 % of the material presenting a half-effect concentration $C_{1/2} \approx 250$ pM and the other 20 % with $C_{1/2} \approx 6$ nM. Considering the major component, the $C_{1/2}$ is about 2,000-fold smaller than found for isolated chromatophores with similar bacteriochlorophyll concentration. We thus have a good agreement between the kinetic and concentration dependence information, which both indicate a vesicle size about 2,000–4,000-fold bigger in spheroplasts compared with isolated chromatophores. A 20 % fraction of the spheroplasts require a higher concentration of gramicidin ($C_{1/2} \approx 6$ nM) to be affected (Fig. 6), suggesting the presence of vesicles with a smaller area. This $C_{1/2}$ is still about two orders of magnitude smaller than found in isolated chromatophores. We did not investigate further the origin of this heterogeneity, which may be a consequence of damage occurring during the preparation.

The fact that the difficulties encountered in cells for gramicidin penetration and the anomalous concentration dependence were eliminated in spheroplasts suggests that the massive sequestration of gramicidin observed in intact cells arises from the outer cell wall, or from the periplasmic content (e.g., the peptidoglycan mesh).

Diffusion potential in intact cells of *Rba. sphaeroides*

If a membrane has a selective permeability to some particular ion, a membrane potential ("diffusion" or Nernst potential) develops when the concentration of this ion differs in the aqueous compartments delimited by the membrane. A popular technique is to use valinomycin as a K^+-channel and impose different KCl concentrations in the external and internal media. Jackson and Crofts (1971) applied this method to chromatophores and could thus compare the carotenoid band-shift generated in this manner

with the light-induced signal. This technique was applied to spheroplasts by Matsuura and Nishimura (1977). Jackson and Crofts (1971) also showed that a proton diffusion potential could be implemented as well, using FCCP as a proton transporter across the membrane. When the pH of the external medium is increased by adding KOH, this creates a temporary gradient of protons, which results (in the presence of proton transporters such as CCCP or FCCP) in a diffusion potential positive on the outside, thus opposite to the light-induced potential. Thanks to the easy permeation of CCCP into cells this method could also be applied to intact cells from *Rhodospirillum molischianum* and *R. photometricum* by Matsuura and Shimada (1993). In the case of spheroplasts or whole cells, the direction of the field with respect to membrane components (as monitored by the carotenoid shift) is opposite to that observed in isolated chromatophores, in agreement with the inverted topology of chromatophores, which close around the periplasmic phase when resealing. Clearly, in the case of cells, the potential generated by this method concerns the cytoplasmic membrane, which separates the external (periplasmic) and internal (cytoplasmic) regions. It will be of no effect on intracytoplasmic vesicles, which can be reached by CCCP, but won't feel the pH gradient. Based on this rationale, we applied this method to intact cells of *Rba. sphaeroides*.

The blue spectrum in Fig. 7 shows the absorption changes caused by the addition of 10 μM FCCP to an aerated suspension of intact cells of *Rba. sphaeroides* in an unbuffered medium containing 100 mM KCl adjusted at pH 6.5. This induced the collapse of the membrane potential and associated carotenoid band-shift generated by the respiratory activity and ATPase activity of the cells. A further addition of KOH, raising the pH to 8.6, induced a carotenoid band-shift with opposite sign, i.e., positive on the periplasmic side of the membrane. Upon addition of KOH into the external medium, a decrease of the outer surface charge of the membrane is expected (due to deprotonation of protein or lipid groups), which counteracts to some extent the diffusion potential of protons. The field sensed by the carotenoid probes will thus be somewhat smaller than predicted on the sole basis of the diffusion potential. Owing to the presence of 100 mM KCl, however, this effect should be relatively small (see Matsuura et al. 1979). The amplitude of the signal (red spectrum in Fig. 7) is similar to that obtained with continuous illumination (see legend), which is expected to develop a similar membrane potential ($\sim$120 mV) to the diffusion potential induced by a pH change by two units. This implies that most of the electrochromic probes are located in the cytoplasmic membrane, rather than in isolated intracytoplasmic vesicles. Similarly, the fact that the amplitude of the respiratory signal collapsed by FCCP addition (squares in Fig. 7) is of the same order (25 % bigger) as the changes induced by light, shows that most of the electrochromic probes (known to be associated with the photosynthetic apparatus) feel the potential generated by the respiratory machinery. Our results are in agreement with the report of Matsuura and Nishimura (1977) who showed that in spheroplasts and in isolated chromatophores of *Rba. sphaeroides* at the same bacteriochlorophyll concentration, the carotenoid shift induced either by light or by a 120 mV diffusion potential had the same amplitude (but with opposite sign as concerns the effect of the diffusion potential in the two types of vesicles).

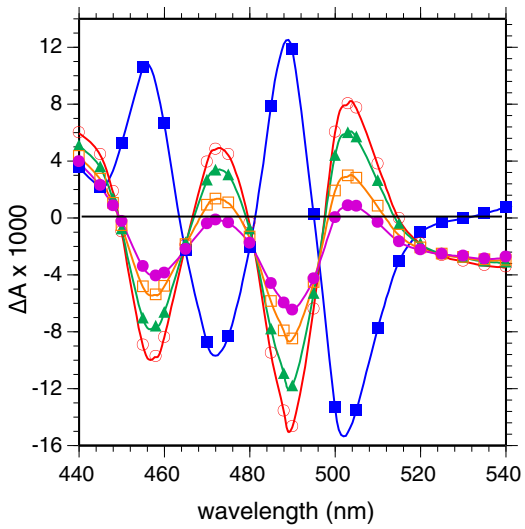

Fig. 7 Difference spectra in the dark, caused by treatments affecting the membrane potential in intact cells of *Rba. sphaeroides* suspended in 100 mM KCl at pH 6.5 under aerobic conditions. The *blue curve* is the difference spectrum induced by the addition of 10 μM FCCP, causing a collapse of the membrane potential sustained by respiration. The other spectra show the changes following the addition of KOH to the medium, causing a pH rise to 8.6. They were obtained by subtracting the spectrum measured before KOH addition (with FCCP present) from spectra acquired at (in order of decreasing amplitude) 20, 80, 230, and 410 s after KOH addition. The decreasing amplitude reflects the collapse of the diffusion potential caused by ionic leaks across the membrane. With the same batch of cells incubated under anaerobic conditions in the absence of any addition, the amplitude of the carotenoid shift (505–490 nm) induced by a saturating continuous illumination was 20.2×10^{-3} absorbance units, thus 75 % of the respiratory signal (*blue spectrum*) or 90 % of the signal induced by the proton diffusion potential (*red spectrum*)

Conclusion

Exploiting the fact that the presence of a single gramicidin channel per vesicle suffices to induce a conspicuous acceleration of the membrane potential decay, we used this ionophore as a probe of the vesicle capacitance (or size) in whole cells. We found that a single channel induces a

decay of the membrane potential with a halftime of about 6 ms, i.e., about 2,000 times longer than the one measured in isolated chromatophores. This implies an area of the functional membrane in intact cells of *Rba. sphaeroides* bigger by about three orders of a magnitude than that of isolated chromatophores. In spheroplasts, the single channel decay half-time was found of the same order of magnitude (23 ms). In this material, the gramicidin concentration at which 50 % of the decay was affected was three orders of magnitude lower than in isolated chromatophores. The slower single channel decay (in intact cells or spheroplasts) and the enhanced sensitivity toward the gramicidin concentration (in spheroplasts) indicate a typical vesicle area about three orders of magnitude larger than that of isolated chromatophores. In whole cells, the concentration dependence could not be used, as it was grossly distorted by a massive sequestration of gramicidin, occurring presumably in the cell wall or in periplasmic material. We also studied the response of intact cells to a diffusion potential caused by a pH jump in the presence of the proton carrier FCCP. This procedure will not affect isolated intracytoplasmic vesicles, but only the membrane in contact with the external medium. The diffusion potential caused by a pH jump of 2 units induced a large electrochromic response of the LH2 carotenoids, with similar amplitude as the light-induced change under saturating illumination, in line with the results of Matsuura and Nishimura (1977) for spheroplasts. These results show that the photosynthetic apparatus is mainly located in the cytoplasmic membrane or in its topologically connected invaginations. As already stated, we noted the absence of any absorbance changes linked to the photo-oxidation of cytochrome c_2 in spheroplasts, suggesting that this protein is mostly present in the periplasmic space (thus liberated into the external medium upon cell wall lysis) rather than in closed intracytoplasmic chromatophores. This is in line with the results of Prince et al. (1975) who found that more than 90 % of *c*-type cytochrome photo-oxidation was lost in *Rba. sphaeroides* spheroplasts.

All these results suggest that most, if not all, of the photosynthetic apparatus is located in a membrane with a size more than three orders of magnitude bigger than the size of a chromatophore, consistent with a topologically continuous ICM. We can estimate a conservative upper limit of about 10 % for the fraction of photosynthetic material that could possibly be located in isolated chromatophores in vivo. For instance, in spheroplasts with 10 nM gramicidin, the fraction of the total signal ascribed to gramicidin-less membranes was about 10 % (Fig. 6). Since vesicles of the chromatophore size should not be significantly affected below 10 nM (Fig. 1, right panel), their possible amount is at most 10 %. Similarly, with whole cells, the largest effect of gramicidin that we obtained (with an addition of 50 μM gramicidin), affected 89 % of the overall signal, inducing a ms decay with no detectable μs contribution (not shown). Again, this leaves at most about 10 % of the total amplitude that could be ascribed to putative isolated chromatophores. A still lower bound can be inferred from the loss of cytochrome c_2 in spheroplasts. We cannot exclude, however, that, as suggested by Niederman (2010), the amount of fully detached vesicles might become significant under growth conditions differing from those used in our study.

To our knowledge, the organization of bioenergetic components within a single continuous membrane appears to be a general rule in photosynthetic bacteria (see e.g., Remsen 1978)—as in chloroplasts and mitochondria. This is clearly the case for bacteria which present no or few invaginations like *Rubrivivax gelatinosus* or lamellar membranes like *Rhodopseudomonas palustris* or tubular membranes like *Thiocapsa pfennigii*. In the complex lamellar architecture of *Phaeospirillum molischianum*, the continuity of the periplasmic space could be evidenced by electron microscopy using the penetration of terbium ions (Mascle-Allemand et al. 2008). The presence of a unique internal membrane may offer several advantages. First of all, a unique membrane does not require a specific distribution of the ATP-synthase, whereas in the case of isolated chromatophores, the presence of at least one ATPase per vesicle would be mandatory. There has been a debate in the literature concerning the abundance of ATP-synthase molecules in isolated chromatophores from *Rba. capsulatus*. According to Feniouk et al. (2002), the average content is about one, implying that a large fraction of vesicles are devoid of ATP-synthase—supporting the sharing of this component in vivo within a membrane of larger size. This was challenged, however, by Gubellini et al. (2007), who found a much higher figure ($\sim$10 ATP-synthase molecules per chromatophore), or Cartron et al. (2014) who found 2 ATPase per chromatophore which would be compatible with the isolated chromatophores scheme. In atomic force microscopy imaging of *Rba. sphaeroides* ICMs, it seems that ATP-synthase was not detected thus far (despite the bulky protrusion of the F_1 component), which would rather support a scarcity of this molecule. Another stake of the overall membrane organization concerns the renewal of the elements of the photosynthetic apparatus, which is bound to be an important issue for a machinery handling excited and radical states. This turnover is clearly much easier to achieve for a unique internal membrane. This is particularly the case for the cytochrome c_2 which requires for its synthesis covalent attachment of the heme to the apocytochrome after their transport across the cytoplasmic membrane. The continuity of the internal membrane and of

the periplasmic space may also be instrumental in allowing a rapid reallocation of the electron carriers common to the different bioenergetic chains both in the membrane (cytochrome bc_1, UQ) and in the periplasm (cytochrome c_2) when the cell has to adapt to changes in its environment. Finally, there may be some advantage in setting a common proton-motive potential in the cell rather than having heterogeneous conditions, as would be the case if a fraction of the photosynthetic chains were present in isolated intracytoplasmic chromatophores and the rest in the cytoplasmic membrane.

Acknowledgment FR acknowledges financial support from the CNRS and the "Initiative d'Excellence" program from the French state (Grant "DYNAMO", ANR-11-LABX-0011-01).

References

Althoff G, Schönknecht G, Junge W (1991) Gramicidin in chromatophores of *Rhodobacter sphaeroides*. Eur Biophys J 19:213–216

Baccarini-Melandri A, Melandri BA (1971) Partial resolution of the photophosphorylation system of *Rhodopseudomonas capsulata*. Methods Enzymol 123:556–561

Béal D, Rappaport F, Joliot P (1999) A new high-sensitivity 10-ns time–resolution spectrophotometric technique adapted to in vivo analysis of the photosynthetic apparatus. Rev Sci Instrum 70:202–207

Cartron ML, Olsen JD, Sener M, Jackson PJ et al (2014) Integration of energy and electron transfer processes in the photosynthetic membrane of *Rhodobacter sphaeroides*. Biochim Biophys Acta 1837:1769–1780

Cohen-Bazire G, Kunisawa R (1962) The fine structure of *Rhodospirillum rubrum*. J Cell Biol 16:401–416

Cotton NPJ, Clark AJ, Jackson JB (1983) Interaction between the respiratory and photosynthetic electron transport chains of intact cells of *Rhodopseudomonas capsulata* mediated by membrane potential. Eur J Biochem 130:581–587

de Rivoyre M, Ginet N, Bouyer P, Lavergne J (2010) Excitation transfer connectivity in different purple bacteria: a theoretical and experimental study. Biochim Biophys Acta 1797:1780–1794

Feniouk BA, Cherepanov DA, Voskoboynikova NE, Mulkidjanian AY, Junge W (2002) Chromatophore vesicles of *Rhodobacter capsulatus* contain on average one F_0F_1-ATP synthase each. Biophys J 82:1115–1122

Frenkel A (1954) Light-induced phosphorylation by cell-free preparations of photosynthetic bacteria. JACS 76:5568–5569

Gubellini F, Francia F, Turina P, Lévy D, Venturoli G, Melandri BA (2007) Heterogeneity of photosynthetic membranes from *Rhodobacter capsulatus*: size dispersion and ATP synthase distribution. Biochim Biophys Acta 1767:1340–1352

Holt SC, Marr AG (1965) Location of chlorophyll in *Rhodospirillum rubrum*. J Bacteriol 89:1402–1412

Hunter CN, Daldal F, Thurnauer MC, Beatty JT (eds) (2009) The purple photosynthetic bacteria. advances in photosynthesis and respiration, vol 28. Springer, Dordrecht

Jackson JB, Crofts AR (1971) The kinetics of light induced carotenoid changes in *Rhodopseudornonas spheroides* and their relation to electrical field generation across the chromatophore membrane. Eur J Biochem 18:120–130

Joliot P, Béal D, Frilley B (1980) Une nouvelle méthode spectrophotométrique destinée à l'étude des réactions photosynthétiques. J Chim Phys 77:209–216

Mascle-Allemand C, Lavergne J, Bernadac A, Sturgis JN (2008) Organisation and function of the *Phaeospirillum molischianum* photosynthetic apparatus. Biochim Biophys Acta 1777:1552–1559

Matsuura K, Nishimura M (1977) Sidedness of membrane structures in *Rhodopseudomonas sphaeroides*: electrochemical titration of the spectrum changes of carotenoid in spheroplasts, spheroplast membrane vesicles and chromatophores. Biochim Biophys Acta 459:483–491

Matsuura K, Shimada (1993) Electrochromic spectral ban shift of carotenoids in the photosynthetic membranes of *Rhodospirillum molischianum* and *Rhodospirillum photometricum*. Biochim Biophys Acta 1140:293–296

Matsuura K, Masamoto K, Itoh S, Nishimura M (1979) Effect of surface potential on the intramembrane electrical field measured with carotenoid spectral shift in chromatophores from *Rhodopseudomonas sphaeroides*. Biochim Biophys Acta 547:91–102

McEwan AG, George CL, Ferguson SJ, Jackson JB (1982) A nitrate reductase activity in *Rhodopseudomonas capsulata* linked to electron transfer and generation of membrane potential. FEBS Lett 150:277–280

McEwan AG, Cotton NPI, Ferguson SJ, Jackson JB (1984) The inhibition of nitrate reduction by light in *Rhodopseudomonas capsulata* is mediated by the membrane potential, but inhibition by oxygen is not. In: Sybesma C (ed) Advances in photosynthesis research, vol 2. Jünk, Nijhoff, Dordrecht, pp 449–452

Nakamura H (1937) Über die Photosynthese bei der schwefelfreiren Purpurbakterie, *Rhodobacillus palustris*. Beitrage zur Stoffwechselphysiologie der Purpurbakterien. Acta Phytochim 9:189–234

Niederman RA (2010) Eukaryotic behaviour of a prokaryotic energy-transducing membrane: fully detached vesicular organelles arise by budding from the *Rhodobacter sphaeroides* intracytoplasmic photosynthetic membrane. Mol Microbiol 76:803–805

Pardee AB, Schachman HK, Stanier RY (1952) Chromatophores of *Rhodospirillum rubrum*. Nature 169:282–283

Prince RC, Baccarini-Melandri A, Hauska GA, Melandri BA, Crofts AR (1975) Asymmetry of an energy transducing membrane: the location of cytochrome c_2 in *Rhodopseudomonas spheroides* and *Rhodopseudomonas capsulata*. Biochim Biophys Acta 387:212–227

Remsen CC (1978) Comparative subcellular architecture of photosynthetic bacteria. In: Clayton RK, Sistrom WR (eds) The photosynthetic bacteria, chapter 3. Plenum Press, New York, pp 31–59

Richaud P, Marrs BL, Verméglio A (1986) Two modes of interaction between photosynthetic and respiratory electron chains in whole cells of *Rhodopseudornonas capsulata*. Biochim Biophys Acta 850:256–263

Rugolo M, Zannoni D (1983) Oxygen-induced inhibition and light-dependent uptake of tetraphenylphosphonium ions as a probe of a direct interaction between photosynthetic and respiratory components in cells of *Rhodopseudomonas capsulata*. Biochem Biophys Res Commun 113:155–162

Sabaty M, Pierre Gans P, Verméglio A (1993) Inhibition of nitrate reduction by light and oxygen in *Rhodobacter sphaeroides* forma sp. *denitrificans*. Arch Microbiol 159:153–159

Satoh T (1977) Light-activated, -inhibited and -independent denitrification by a denitrifying phototrophic bacterium. Arch Microbiol 115:293–298

Scheuring S, Nevo R, Li L-N, Mangenot S, Dana Charuvi D, Boudier T, Prima V, Hubert P, Sturgis JN, Reich Z (2014) The architecture of *Rhodobacter sphaeroides* chromatophores. Biochim Biophys Acta 1837:1263–1270

Tucker JD, Siebert CA, Escalante M, Adams PG et al (2010) Membrane invagination in *Rhodobacter sphaeroides* is initiated at curved regions of the cytoplasmic membrane, then forms both budded and fully detached spherical vesicles. Mol Microbiol 76:833–847

van Niel CB (1941) The bacterial photosynthesis and their importance for the general problem of photosynthesis. Adv Enzymol 1:263–318

Vatter AE, Wolfe RS (1958) The structure of photosynthetic bacteria. J Bacteriol 75:480–488